Hyperfluorescence

DOI: 10.1002/anie.201402992

Luminous Butterflies: Efficient Exciton Harvesting by Benzophenone Derivatives for Full-Color Delayed Fluorescence OLEDs**

Sae Youn Lee, Takuma Yasuda, Yu Seok Yang, Qisheng Zhang, and Chihaya Adachi**

Abstract: *Butterfly-shaped luminescent benzophenone derivatives with small energy gaps between their singlet and triplet excited states are used to achieve efficient full-color delayed fluorescence. Organic light-emitting diodes (OLEDs) with these benzophenone derivatives doped in the emissive layer can generate electroluminescence ranging from blue to orange–red and white, with maximum external quantum efficiencies of up to 14.3 %. Triplet excitons are efficiently harvested through delayed fluorescence channels.*

Organic molecules exhibiting strong visible-light emission continue to receive considerable attention because of their promising application in organic light-emitting diodes (OLEDs)[1] and as bioimaging probes.[2] The technological prospects for full-color flat-panel displays and solid-state lighting sources have driven the development of red, green, and blue (RGB) light-emitting materials with high luminescence quantum efficiencies.[3] The discovery of phosphorescent materials containing heavy transition metals, such as iridium(III) and platinum(II), was a major breakthrough towards high-performance OLEDs.[4] According to spin statistics, 75 % triplet (T_1) and 25 % singlet (S_1) excitons are formed by the recombination of a hole and an electron under electrical excitation. In conventional fluorescent organic materials, only up to 25 % of the total electro-generated excitons can be used for light emission. In contrast, both S_1 and T_1 excitons can be harvested in phosphorescent organometallic materials, as the strong spin-orbit coupling of the heavy-metal center enhances intersystem crossing (ISC). This results in nearly 100 % electron-to-photon conversion efficiency in phosphorescent OLEDs.[5] However, these phosphorescent materials suffer from instability in practical applications, especially for blue and white emission. The expense and rarity of precious-metal complexes also limits their cost effectiveness and long-term mass production. Realizing high-efficiency RGB electroluminescence (EL) through a simple organic system while aiming to reduce production costs and simplify manufacturing processes is pivotal for next-generation OLED technology.

We recently explored an alternative approach to harvest excited triplet energy through upconversion from the T_1 to S_1 states by thermal activation, giving rise to thermally activated delayed fluorescence (TADF),[6–10] without using precious-metal complexes. For efficient TADF emission, a very small energy gap (ΔE_{ST}) between the S_1 and T_1 states is required to promote reverse intersystem crossing (RISC) and harvest formally spin-forbidden T_1 excitons. We, and others, have developed various TADF pure organic luminophores[6–10] and copper(I) complexes,[11] with small ΔE_{ST} values with high radiative decay rates. However, the basic molecular frameworks for organic TADF molecules remain limited to azaheteroaromatics (e.g. triazines[6] and oxadiazoles[7]), cyanobenzenes,[8] sulfones,[9] and spirofluorene derivatives.[10] Thus, the challenge is to rationally design novel families of TADF luminophores based on simple versatile molecular scaffolds which exhibit emission across the entire visible range.

Herein, we report a series of butterfly-shaped TADF-emitting benzophenones featuring donor–acceptor–donor (D-A-D) electronic configurations (Figure 1). Benzophenone itself was previously explored as an emitter in OLEDs,[12] because of its phosphorescence and efficient intersystem

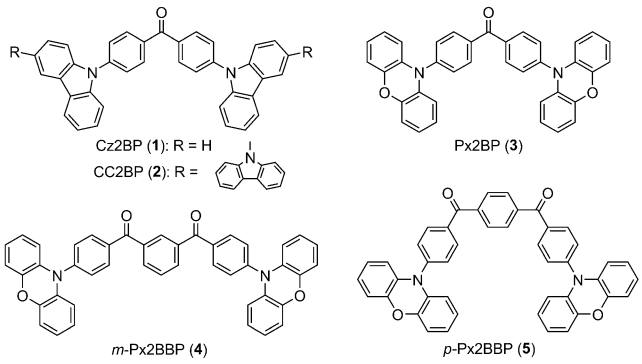

Figure 1. Structural formulae of the butterfly-shaped benzophenone derivatives **1**–**5**.

[*] S. Y. Lee, Prof. Dr. T. Yasuda, Dr. Y. S. Yang, Dr. Q. Zhang, Prof. Dr. C. Adachi
Department of Applied Chemistry and Center for Organic Photonics and Electronics Research (OPERA), Kyushu University
744 Motooka, Nishi-ku, Fukuoka 819-0395 (Japan)
E-mail: yasuda@cstf.kyushu-u.ac.jp
adachi@cstf.kyushu-u.ac.jp
Homepage: http://www.cstf.kyushu-u.ac.jp/~adachilab/
Prof. Dr. T. Yasuda, Prof. Dr. C. Adachi
International Institute for Carbon Neutral Energy Research (WPI-I2CNER), Kyushu University
744 Motooka, Nishi-ku, Fukuoka 819-0395 (Japan)
Prof. Dr. T. Yasuda
PRESTO (Japan) Science and Technology Agency (JST)
Chiyoda-ku, Tokyo 102-0076 (Japan)

[**] This work was supported by a Grant-in-Aid from the Funding Program for World-Leading Innovation R&D on Science and Technology (FIRST), Precursory Research for Embryonic Science and Technology (PRESTO) from JST (no. 10111), and from JSPS Young Scientist (A) (no. 25708032). C.A. and T.Y. acknowledge the support of WPI-I2CNER, sponsored by MEXT (Japan).
OLEDs = organic light-emitting diodes.

Supporting information for this article is available on the WWW under http://dx.doi.org/10.1002/anie.201402992.

crossing.[13] To our knowledge, however, practical EL from benzophenone derivatives at ambient temperature has not been detected. A remarkable feature of our system is that OLEDs employing benzophenones with a D-A-D structure as light-emitting centers can generate highly efficient blue to orange–red TADF by upconversion. The external EL quantum efficiencies of these systems greatly exceed the theoretical limit of conventional fluorescence OLEDs.

The syntheses of the benzophenone derivatives **1**–**5** were accomplished using Buchwald–Hartwig aminations of 4,4′-dibromobenzophenone or bis(4-bromobenzoyl)benzenes with two equivalents of the corresponding donor units (carbazole to prepare **1**, bicarbazole for **2**, and phenoxazine for **3**–**5**) in high yields (84–96%) by employing a $[Pd(tBu_3P)_2]/K_2CO_3$ catalytic system. Detailed synthetic procedures and characterization data for compounds **1**–**5** are described in the Supporting Information.

In principle, ΔE_{ST} should decrease upon decreasing the exchange interaction integral of the HOMO and LUMO wavefunctions of a molecule.[14] Consequently, careful selection of appropriate donor units is crucial to form full-color TADF molecules, with their HOMO and LUMO being localized on different constituents. To gain insight into the geometric and electronic structures of **1**–**5**, time-dependent density functional theory (TD-DFT) calculations were performed at the B3LYP/6-31G(d,p) level. The transition energies, oscillator strengths, and assignments for the most relevant singlet and triplet excited states for compounds **1**–**5** are provided in Table S1 (Supporting Information). All molecules exhibit clear separation of the HOMO and LUMO distributions. As shown in Figure 2, for compounds **1**–**3** the LUMO is predominantly located on the central electron-accepting benzophenone core, whereas the HOMO is mainly localized on the electron-donating peripheral carbazole or phenoxazine substituents, because of the highly twisted geometry between the donor and acceptor constituents. In their optimized ground-state geometries, the dihedral angles between the phenyl rings of the benzophenone unit and adjacent carbazoles are calculated to be 51° for compound **1** and 61° for **2**, and for **3** with phenoxazines to be 85°. This clear separation of the frontier orbitals leads to small calculated ΔE_{ST} values of 0.01–0.32 eV (Table 1), and suggests that excitons may be harvested by $T_1 \rightarrow S_1$ upconversion. All investigated lowest-energy excited states correspond to an

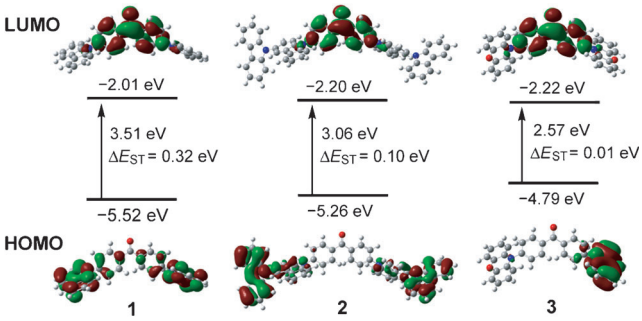

Figure 2. Frontier-molecular-orbital distributions, energy levels and energy gaps (ΔE_{ST}) between S_1 and T_1 for compounds **1**–**3**, characterized by TD-DFT calculations.

intramolecular charge transfer (ICT) with a small exchange energy and are mainly described by the HOMO→LUMO transition (Table S1). The S_1 states for **1** and **2** have relatively large oscillator strengths ($f = 0.36$ and 0.15, respectively). The oscillator strength for the electronic transition tends to decrease upon substitution with more sterically-hindered phenoxazine donor units ($f = 0.01$–0.02 for compounds **3**–**5**).

Consistent with the quantum chemical calculations, tuning of emission color can be observed with the naked eye; compounds **1**–**5** exhibit bright photoluminescence (PL) in solution, with emission color varying from blue to green, and orange–red (Figure 3a). This suggests that changing the degree of ICT effectively modulates the emission wavelength of the molecules. Steady-state UV/Vis absorption and PL spectra of compounds **1**–**5** in toluene are depicted in Figure 3b, and the photophysical data are summarized in Table 1. In oxygen-free toluene solution, compounds **1**–**5** exhibited broad structureless emission with PL quantum yields (Φ_{PL}) of 10–44%; whilst the PL intensity drastically decreased in the presence of triplet oxygen ($^3O_2$) in aerated solutions. From compound **1**, with carbazole donor units, to **3**, with phenoxazine units, the PL emission peak (λ_{PL}) is red-shifted by 71 nm. Depending on the substitution mode of an additional benzoyl group on the innermost benzene ring, considerable red shifts of λ_{PL} were observed in the PL spectra of bis(benzoyl)benzenes **4** ($\lambda_{PL} = 566$ nm) and **5** ($\lambda_{PL} = 600$ nm) in solution, when compared with **3** ($\lambda_{PL} = 509$ nm). This suggests that the additional electron-withdrawing benzoyl unit with the *para*-linkage (compound **5**) stabilizes the

Table 1: Photophysical properties of the benzophenone-based TADF luminophores **1**–**5**.

Compound	λ_{abs} [nm] sol[a]	λ_{PL} [nm] sol[a]/film[b]	Φ_{PL} [%][c] sol[a]/film[b]	τ_p (Φ_F) [ns (%)][d]	τ_d (Φ_{TADF}) [μs (%)][d]	HOMO [eV][e]	LUMO [eV][f]	E_S/E_T [eV][g]	ΔE_{ST} [eV][h]	calc. ΔE_{ST} [eV][i]
Cz2BP (**1**)	340, 353[j]	438/444	21/55	59(5)	710(50)	−5.74	−2.64	3.10/2.89	0.21	0.32
CC2BP (**2**)	345	462/475	38/73	62(11)	460(62)	−5.65	−2.63	3.02/2.88	0.14	0.10
Px2BP (**3**)	324, 413	509/538	44/70	23(41)	12(29)	−5.44	−2.92	2.61/2.58	0.03	0.01
m-Px2BBP (**4**)	324, 416	566/541(575)	36/71(29)	24(44)	13(27)	−5.64	−3.03	2.62/2.52	0.10	0.02
p-Px2BBP (**5**)	322, 425	600/555	10/36	26(26)	2.9(10)	−5.62	−3.13	2.59/2.53	0.06	0.02

[a] Measured in oxygen-free toluene solution at room temperature. [b] 6 wt%-doped film in a host matrix (host = DPEPO for **1** and **2**; mCP for **3**; mCBP for **4** and **5**). The data for a neat film are given in parentheses. [c] Absolute PL quantum yield evaluated using an integrating sphere. [d] PL lifetimes of prompt (τ_p) and delayed (τ_d) decay components for the 6 wt%-doped film measured at 300 K under vacuum. The fractional contributions of fluorescence (Φ_F) and TADF (Φ_{TADF}) to the total Φ_{PL} [%] are given in parentheses. [e] Determined by photoelectron yield spectroscopy in thin films. [f] Deduced from the HOMO and optical energy gap (E_g). [g] Singlet (E_S) and triplet (E_T) energies estimated from onset wavelengths of the doped film emission spectra at 300 and 5 K, respectively. [h] $\Delta E_{ST} = E_S - E_T$. [i] Calculated by TD-DFT at B3LYP/6-31G(d,p). [j] Shoulder peak.

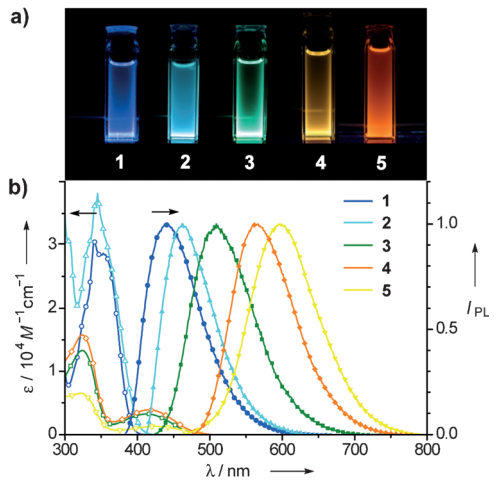

Figure 3. a) Luminescence images of compounds **1**–**5** in toluene solutions recorded under UV irradiation (λ_{ex} = 365 nm). b) Absorption (left) and normalized PL (right) spectra of compounds **1**–**5** in toluene at room temperature.

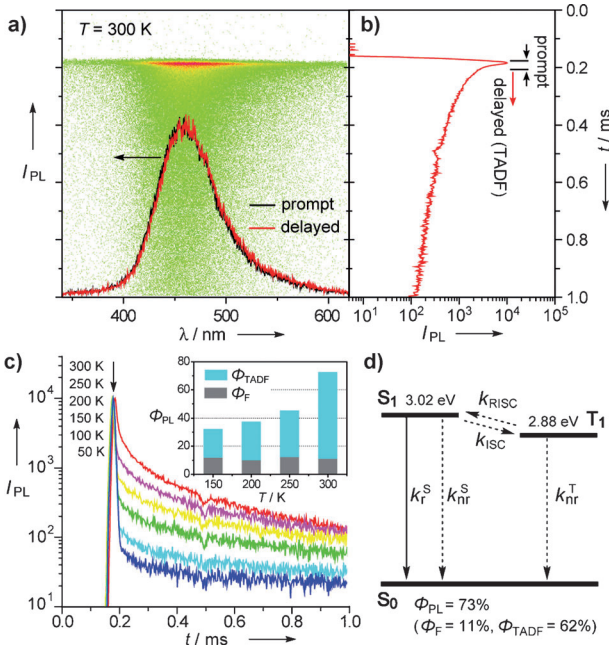

Figure 4. a) Streak image and corresponding time-dependent emission spectra, and b) transient PL decay profile of a **2**(6 wt%):DPEPO codeposited film recorded at 300 K. Prompt fluorescence (black) and TADF (red) components are shown. Each dot in the streak image represents a PL photon count. c) Temperature dependence of transient PL decay. Inset: the fractional contribution of fluorescence and TADF to the total PL quantum yield (Φ_{PL}). d) Schematic representation of PL decay of **2**. k_r^S and k_{nr}^S are the radiative and non-radiative decay rate constants of the S_1 state, respectively, k_{ISC} and k_{RISC} are the ISC ($S_1 \rightarrow T_1$) and RISC ($T_1 \rightarrow S_1$) rate constants, respectively, and k_{nr}^T is the non-radiative rate constant of the T_1 state.

LUMO, resulting in a decreased bandgap energy compared with *meta*-linked compound **4**. Thus, fine tuning of the luminescence properties is achieved by simple chemical modification of benzophenone.

To better understand the nature of the emitting states, the transient PL characteristics and temperature dependence were analyzed using a streak camera (Figure 4). We focused on host:guest solid thin films containing low concentrations of the guest emitters **1**–**5**, to avoid concentration quenching of the emitter and complications by solvent phase changes. For the blue emitters **1** and **2**, bis[2-(diphenylphosphino) phenyl]ether oxide (DPEPO)[15] with higher S_1 and T_1 energies (E_S/E_T = 3.5/3.1 eV) was selected as a host to prevent the backward excited energy transfer from the guest to host. The Φ_{PL} for compounds **1**–**5** in suitable amorphous host matrices are approximately two- to three-times larger than those measured in dilute solutions (Table 1). This result is because of reduced non-radiative relaxation as intramolecular torsional/vibrational motions are restricted in the solid state.[16]

The results displayed in Figure 4 for a **2**(6 wt%):DPEPO codeposited film indicate two-component emission decays, consisting of a nanosecond-scale prompt component (lifetime τ_p = 62 ns) and a microsecond-scale delayed component (τ_d = 460 μs) at 300 K. As the delayed emission has the same spectral profile as normal fluorescence from the S_1 state but with a longer decay time, the long-lived emission can be assigned to TADF. Furthermore, the TADF emission intensity is found to increase with increasing temperature from 50 to 300 K (Figure 4c). At ambient temperature (300 K), the upper-lying S_1 state is significantly populated by thermally activated upconversion from the T_1 state, and in turn emits efficient TADF. Hence, the overall Φ_{PL} of the **2**:DPEPO-doped film reaches 73 ± 2% at room temperature, which includes quantum efficiencies of 11 ± 2% for fluorescence (Φ_F) and 62 ± 2% for TADF (Φ_{TADF}), as listed in Table 1. Using the PL efficiency and lifetime data measured at 300 K, the radiative decay rate constant of the S_1 state (k_r^S), the ISC rate constant (k_{ISC}), and the RISC rate constant (k_{RISC}) of **2** in the doped film are estimated to be approximately $1–2 \times 10^6$, $1–2 \times 10^7$, and $1–2 \times 10^4\ s^{-1}$, respectively (Figure 4d, see Supporting Information for details).

The photophysical properties of the D-A-D-structured benzophenones with high Φ_{TADF} values of approximately 36–73% in their doped films are favorable for developing highly efficient OLEDs. To evaluate the performance of **1**–**5** as emitters, multilayer OLED devices **A**–**E** were fabricated (see Figure 5 for device configurations). Devices **A** and **B** had compounds **1** and **2**, respectively, as emitters, and devices **C**–**E** had compounds **3**–**5** as emitters. The compound 4,4′-bis[*N*-(1-naphthyl)-*N*-phenylamino]-1,1′-biphenyl (α-NPD) was employed as a hole-transporting layer (HTL) and 1,3,5-tris(*N*-phenylbenzimidazol-2-yl)benzene (TPBi) as an electron-transporting layer (ETL). For devices **A** and **B**, thin layers of 1,3-bis(carbazol-9-yl)benzene (mCP) and DPEPO with sufficiently high E_T were inserted at the emitting layer/HTL and ETL interfaces, respectively, to confine T_1 excitons in the blue-emitting molecules, and suppress T_1 exciton quenching. For the orange–red-emitting device **E**, compound **4** was used as a non-doped light-emitting layer. The energy-level diagrams of the devices and structural formulae of their materials are provided in the Supporting Information.

Figure 5 presents external EL quantum efficiency (η_{ext}) versus current-density plots, current-density–voltage (*J*–*V*) characteristics, and EL spectra of the fabricated devices. The

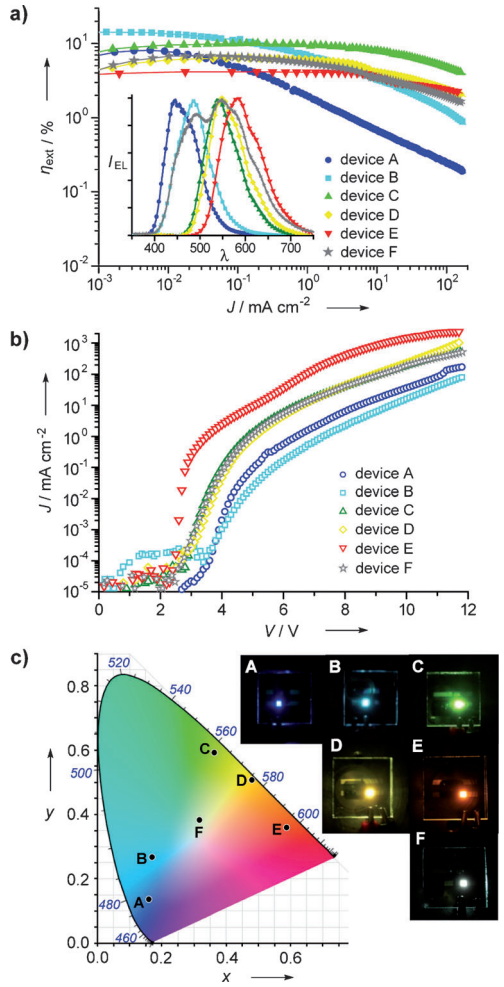

Figure 5. a) External EL quantum efficiency (η_{ext}) versus current-density plots (inset: normalized EL spectra measured at 10 mA cm^{-2}, λ/nm) and b) current-density–voltage (J–V) curves of the OLEDs **A**–**F** containing the TADF emitters **1**–**5**. c) EL emission color coordinates in the CIE 1931 chromaticity diagram and photographs of devices **A**–**F**. Device configurations: for **A** and **B**, ITO/α-NPD (35 nm)/mCP (5 nm)/ **1** or **2**(6 wt%):host (20 nm)/DPEPO (10 nm)/TPBi (30 nm)/LiF (0.8 nm)/Al (80 nm); for **C** and **D**, ITO/α-NPD (40 nm)/ **3** or **5**(6 wt%):host (20 nm)/TPBi (40 nm)/LiF (0.8 nm)/Al (80 nm); for **E**, ITO/α-NPD (40 nm)/**4** (neat, 20 nm)/TPBi (40 nm)/LiF (0.8 nm)/Al (80 nm); for **F**, ITO/α-NPD (35 nm)/**5**(18 wt%):mCBP (4 nm)/**2**(6 wt%):PPF (14 nm)/PPF (40 nm)/LiF (0.8 nm)/Al (80 nm).

Table 2: TADF-OLED performance of the devices **A**–**F**[a].

Device	A	B	C	D	E	F
Emitter	**1**	**2**	**3**	**5**	**4**	**2**/**5**
Host	DPEPO	DPEPO	mCP	mCBP	none	PPF/mCPB
λ_{EL} [nm]	446	484	539	548	586	489/548
V_{on} [V]	4.3	4.4	3.2	3.6	2.8	5.0
L_{max} [cd m^{-2}]	510	3900	86100	57120	50820	9800
η_c [cd A^{-1}]	9.3	25.5	35.9	20.1	11.1	16.4
η_{ext} [%]	8.1	14.3	10.7	6.9	4.2	6.7
CIE [x, y]	0.16, 0.14	0.17, 0.27	0.37, 0.58	0.49, 0.51	0.58, 0.36	0.32, 0.39

[a] Abbreviations: λ_{EL} = EL emission maximum, V_{on} = turn-on voltage at 1 cd m^{-2}, L_{max} = maximum luminance, η_c = maximum current efficiency, η_{ext} = maximum external EL quantum efficiency (at L > 1 cd m^{-2}), CIE = Commission Internationale de l'Éclairage color coordinates measured at 10 mA cm^{-2}, DPEPO = bis[2-(diphenylphosphino)phenyl]ether oxide, mCP = 1,3-bis(carbazol-9-yl)benzene, mCBP = 3,3′-bis(carbazol-9-yl)biphenyl, PPF = 2,8-bis(diphenylphosphoryl)dibenzo[*b*,*d*]furan.

key characteristics are summarized in Table 2. All devices based on **1**–**5** exhibited EL spectra similar to the corresponding PL spectra of their doped (or neat) films (Figure 5a), confirming that EL emission was generated solely from the emitters themselves, through the same radiative decay process. As illustrated in a Commission Internationale de l'Éclairage (CIE) chromaticity diagram in Figure 5c, the EL emission color can be tuned from blue (0.16, 0.14; device **A**) to orange–red (0.58, 0.36; device **E**) using the TADF benzophenones **1**–**5**.

The sky-blue-emitting device **B** containing emitter **2** achieved a high maximum η_{ext} of 14.3% and current efficiency (η_c) of 25.5 cd A^{-1} at low current densities. With increasing current density, the η_{ext} of device **B** and blue-emitting device **A** decrease more rapidly than for the other devices. This efficiency roll-off at high current density is mainly attributed to excess T_1 excitons in the emitting layer, which cause exciton quenching by triplet–triplet and/or singlet–triplet annihilation.[17] The green-emitting device **C** incorporating emitter **3** also displayed notable EL efficiencies, with a η_{ext} measuring 10.7%, a η_c of 35.9 cd A^{-1}, and a high maximum luminance (L_{max}) of 86100 cd m^{-2}. At a high current density of 100 mA cm^{-2}, the η_{ext} value of device **C** was still as high as 5%, indicating a reduced efficiency roll-off, presumably because of the relatively short TADF lifetime (12 μs) for the doped film of **3**. Although the performances of the blue-emitting device **A** and yellow-emitting device **D** were lower than that of device **C**, maximum η_{ext} values of 8.1% and 6.9% were obtained, respectively, which are much higher than the 5% theoretical limit for the η_{ext} of conventional fluorescence OLEDs.

The combination of these TADF benzophenones with emission wavelengths spanning the whole visible region should allow TADF-based white OLEDs to be fabricated. There are two approaches for generating white light from OLEDs: three primary-color (RGB) and two-color (blue/yellow) emitting systems. Because of the simpler device fabrication process, we adopted a two-color-based device configuration (device **F**) with ITO/α-NPD (35 nm)/ **5**-(18 wt%):mCBP (4 nm)/**2**(6 wt%):PPF (14 nm)/PPF (40 nm)/LiF (0.8 nm)/Al (80 nm), in which **2** and **5** function as sky-blue and yellow emitters, respectively. As expected, device **F** emitted white EL with CIE coordinates of (0.32, 0.39), which are close to those of pure white light CIE (0.33, 0.33), and achieved a η_{ext} of 6.7% (Table 2). The resulting EL spectrum exhibited component peaks at λ = 489 and 548 nm, corresponding to emission from **2** and **5**, respectively (see Figure 5a inset).

The η_{ext} for OLEDs is generally expressed by Equation (1):

$$\eta_{ext} = \eta_{int}\,\eta_{out} = \gamma\,\eta_{ST}\,\Phi_{PL}\,\eta_{out} \qquad (1)$$

where, η_{int} is the internal EL quantum efficiency, η_{out} is the light out-coupling efficiency (typically

around 20%, which is derived from $1-(1-1/n^2)^{1/2}$, where n is the refractive index of the organic layers),[18] γ is the charge balance factor (ideally $\gamma \approx 1$ if holes and electrons are fully balanced and recombine to generate excitons), η_{ST} is the fraction of radiative excitons ($\eta_{ST} = 0.25$ for conventional fluorescent emitters, according to the classical spin degeneracy statistics of 1:3 for singlet-to-triplet excitons), and Φ_{PL} is the quantum yield of the emitting layer. Considering the measured Φ_{PL} values of **1**–**5** (see Table 1), greatly enhanced η_{ST} efficiencies of 72–98% are estimated for devices **A**–**E**. Note, the maximum η_{ST} of **2** (98%) is nearly four times higher than the 25% limit of spin statistical ratio for conventional fluorescent materials.

In conclusion, efficient exciton-harvesting through spin upconversion from non-radiative T_1 to radiative S_1 states has been realized, using butterfly-shaped benzophenone derivatives. Our results demonstrate that the judicious molecular design of benzophenone based on D-A-D frameworks is valid for the production of organic luminophores exhibiting highly efficient full-color TADF emissions. OLEDs employing the benzophenone derivatives as emitters have achieved maximum external quantum efficiencies of up to 14.3%, which far exceed the theoretical limit for conventional fluorescence OLEDs. These purely organic luminophores do not require expensive precious metals, in contrast to phosphorescent emitters, and will therefore benefit large-area applications. Continued exploration of similar materials offers a viable route for producing efficient and stable full-color TADF luminophores for future display and lighting applications.

Received: March 4, 2014
Published online: May 18, 2014

Keywords: benzophenone · donor–acceptor systems · organic light-emitting diodes · organic semiconductors · photochemistry

[1] a) *Organic Light-Emitting Devices: Synthesis Properties and Applications* (Eds.: K. Müllen, U. Scherf), Wiley-VCH, Weinheim, **2006**; b) *Highly Efficient OLEDs with Phosphorescent Materials* (Ed.: H. Yersin), Wiley-VCH, Weinheim, **2008**.

[2] For recent Reviews, see: a) J. Chan, S. C. Dodani, C. J. Chang, *Nat. Chem.* **2012**, *4*, 973–984; b) L. Yuan, W. Lin, K. Zhang, S. Zhu, *Acc. Chem. Res.* **2013**, *46*, 1462–1473; c) Z. Guo, S. Park, J. Yoon, I. Shin, *Chem. Soc. Rev.* **2014**, *43*, 16–29.

[3] a) B. W. D'Andrade, S. R. Forrest, *Adv. Mater.* **2004**, *16*, 1585–1595; b) M. C. Gather, A. Köhnen, K. Meerholz, *Adv. Mater.* **2011**, *23*, 233–248; c) K. T. Kamtekar, A. P. Monkman, M. R. Bryce, *Adv. Mater.* **2010**, *22*, 572–582; d) H. Sasabe, J. Kido, *Chem. Mater.* **2011**, *23*, 621–630.

[4] a) M. A. Baldo, D. F. O'Brien, Y. You, A. Shoustikov, S. Sibley, M. E. Thompson, S. R. Forrest, *Nature* **1998**, *395*, 151–154; b) M. A. Baldo, S. Lamansky, P. E. Burrows, M. E. Thompson, S. R. Forrest, *Appl. Phys. Lett.* **1999**, *75*, 4–6; c) S. Lamansky, P. Djurovich, D. Murphy, F. Abdel-Razzaq, H.-E. Lee, C. Adachi, P. E. Burrows, S. R. Forrest, M. E. Thompson, *J. Am. Chem. Soc.* **2001**, *123*, 4304–4312; d) J. Brooks, Y. Babayan, S. Lamansky, P. I. Djurovich, I. Tsyba, R. Bau, M. E. Thompson, *Inorg. Chem.* **2002**, *41*, 3055–3066.

[5] a) C. Adachi, M. A. Baldo, M. E. Thompson, S. R. Forrest, *J. Appl. Phys.* **2001**, *90*, 5048–5051; b) C. Adachi, M. A. Baldo, S. R. Forrest, M. E. Thompson, *Appl. Phys. Lett.* **2000**, *77*, 904–906; c) L. Xiao, S.-J. Su, Y. Agata, H. Lan, J. Kido, *Adv. Mater.* **2009**, *21*, 1271–1274.

[6] a) S. Y. Lee, T. Yasuda, H. Nomura, C. Adachi, *Appl. Phys. Lett.* **2012**, *101*, 093306; b) A. Endo, K. Sato, K. Yoshimura, T. Kai, A. Kawada, H. Miyazaki, C. Adachi, *Appl Phys. Lett.* **2011**, *98*, 083302; c) K. Sato, K. Shizu, K. Yoshimura, A. Kawada, H. Miyazaki, C. Adachi, *Phys. Rev. Lett.* **2013**, *110*, 247401; d) H. Tanaka, K. Shizu, H. Miyazaki, C. Adachi, *Chem. Commun.* **2012**, *48*, 11392–11394.

[7] J. Lee, K. Shizu, H. Tanaka, H. Nomura, T. Yasuda, C. Adachi, *J. Mater. Chem. C* **2013**, *1*, 4599–4604.

[8] a) H. Uoyama, K. Goushi, K. Shizu, H. Nomura, C. Adachi, *Nature* **2012**, *492*, 234–238; b) T. Nishimoto, T. Yasuda, S. Y. Lee, R. Kondo, C. Adachi, *Mater. Horiz.* **2014**, *1*, 264–269.

[9] a) Q. Zhang, J. Li, K. Shizu, S. Huang, S. Hirata, H. Miyazaki, C. Adachi, *J. Am. Chem. Soc.* **2012**, *134*, 14706–14709; b) F. B. Dias, K. N. Bourdakos, V. Jankus, K. C. Moss, K. T. Kamtekar, V. Bhalla, J. Santos, M. R. Bryce, A. P. Monkman, *Adv. Mater.* **2013**, *25*, 3707–3714.

[10] a) G. Méhes, H. Nomura, Q. Zhang, T. Nakagawa, C. Adachi, *Angew. Chem.* **2012**, *124*, 11473–11477; *Angew. Chem. Int. Ed.* **2012**, *51*, 11311–11315; b) K. Nasu, T. Nakagawa, H. Nomura, C.-J. Lin, C.-H. Cheng, M.-R. Tseng, T. Yasuda, C. Adachi, *Chem. Commun.* **2013**, *49*, 10385–10387.

[11] a) J. C. Deaton, S. C. Switalski, D. Y. Kondakov, R. H. Young, T. D. Pawlik, D. J. Giesen, S. B. Harkins, A. J. M. Miller, S. F. Mickenberg, J. C. Peters, *J. Am. Chem. Soc.* **2010**, *132*, 9499–9508; b) R. Czerwieniec, J. Yu, H. Yersin, *Inorg. Chem.* **2011**, *50*, 8293–8301; c) H. Yersin, A. F. Rausch, R. Czerwieniec, T. Hofbeck, T. Fischer, *Coord. Chem. Rev.* **2011**, *255*, 2622–2652; d) R. Czerwieniec, K. Kowalski, H. Yersin, *Dalton Trans.* **2013**, *42*, 9826–9830.

[12] a) S. Hoshino, H. Suzuki, *Appl. Phys. Lett.* **1996**, *69*, 224–226, and references therein; b) T. Tsutsui, C. Adachi, S. Saito in *Photochemical Processes in Organized Molecular Systems* (Ed.: K. Honda), Elsevier, Amsterdam, **1991**, pp. 437–450.

[13] a) M. W. Wolf, K. D. Legg, R. E. Brown, L. A. Singer, J. H. Parks, *J. Am. Chem. Soc.* **1975**, *97*, 4490–4497; b) Y.-P. Sun, D. F. Sears, Jr., J. Saltiel, *J. Am. Chem. Soc.* **1989**, *111*, 706–711; c) S. Aloïse, C. Ruckebusch, L. Blanchet, J. Réhaut, G. Buntinx, J.-P. Huvenne, *J. Phys. Chem. A* **2008**, *112*, 224–231.

[14] N. J. Turro, V. Ramamurthy, J. C. Scaiano, *Modern Molecular Photochemistry of Organic Molecules*, University Science Books, Sausalito, **2010**.

[15] a) Q. Zhang, T. Komino, S. Huang, S. Matsunami, K. Goushi, C. Adachi, *Adv. Funct. Mater.* **2012**, *22*, 2327–2336; b) C. Han, Y. Zhao, H. Xu, J. Chen, Z. Deng, D. Ma, Q. Li, P. Yan, *Chem. Eur. J.* **2011**, *17*, 5800–5803.

[16] a) Y. Liu, S. Chen, J. W. Y. Lam, P. Lu, R. T. K. Kwok, F. Mahtab, H. S. Kwok, B. Z. Tang, *Chem. Mater.* **2011**, *23*, 2536–2544; b) C. Y. K. Chan, Z. Zhao, J. W. Y. Lam, J. Liu, S. Chen, P. Lu, F. Mahtab, X. Chen, H. H. Y. Sung, H. S. Kwok, Y. Ma, I. D. Williams, K. S. Wong, B. Z. Tang, *Adv. Funct. Mater.* **2012**, *22*, 378–389; c) B.-K. An, S.-K. Kwon, S.-D. Jung, S. Y. Park, *J. Am. Chem. Soc.* **2002**, *124*, 14410–14415; d) J. Y. Kim, T. Yasuda, Y. S. Yang, C. Adachi, *Adv. Mater.* **2013**, *25*, 2666–2671; e) R. Kondo, T. Yasuda, Y. S. Yang, J. Y. Kim, C. Adachi, *J. Mater. Chem.* **2012**, *22*, 20689–20695.

[17] a) Y. Zhang, S. R. Forrest, *Phys. Rev. Lett.* **2012**, *108*, 267404; b) C. Adachi, M. A. Baldo, S. R. Forrest, *J. Appl. Phys.* **2000**, *87*, 8049.

[18] B. E. A. Saleh, M. C. Teich, *Fundamentals of Photonics*, 2nd ed., Wiley, New York, **2007**.

